Accelerometric radiation simulation for the September 26, 1997 Umbria-Marche (Central Italy) main shocks

Antonio Emolo and Aldo Zollo
Dipartimento di Scienze Fisiche, Università «Federico II», Napoli, Italy

Abstract
We applied a hybrid stochastic-deterministic method to simulate the strong ground motion characteristics associated with the September 26, 1997 Umbria-Marche main shocks. One hundred different rupture processes on previously inferred fault planes were simulated. The maps of computed PGA (mean values from 100 simulations) show a SE alignment for the 00:33 event and a NW alignment for the 09:40 event, in accordance with the macroseismic data. Moreover, we found a good agreement between the predicted 1σ interval for the PGA values and the data recorded at several accelerometric stations. As a further test, we computed the response spectra at the station Cerreto di Spoleto and found a satisfactory agreement with the synthetic results.

Key words *kinematic source model – strong motion simulation – Umbria-Marche main shocks*

1. Introduction

The predictive estimate of strong motion parameters (Peak Ground Acceleration/Velocity, PGA and PGV, and spectral ordinates) of engineering interest provides a quantitative characterization of seismic hazard in an active seismic area. Seismic hazard is generally estimated by using probabilistic description of seismicity and empirical relationships between magnitude and PGA as a function of epicentral distance. Most of these relations take into account only the average characteristics of the earthquake source processes and seismic wave propagation. They generally give satisfactory estimates for sufficiently large source-to-receiver distances although recent updated databases can be used to predict strong motion parameters at smaller distances (Abrahamson and Shedlock, 1997; Boore *et al.*, 1997). In the near source range (distance between source and receivers comparable with the fault dimensions) the details of rupture process may largely influence the high frequency seismic radiation. Moreover, the heterogeneous final slip and rupture velocity distributions on the fault plane are rather complex, as seen from near source strong motion data (Hartzell and Heaton, 1983; Heaton, 1990). The complexity of the rupture process can be related to the variable rock strength and/or applied stress field along the faulting surface.

Recent paleoseismic evidence of the occurrence of repeated rupture episodes along the same fault (or fault system) suggests that some characteristics like fault geometry, the source mechanism and the average slip, depend on the direction and intensity of regional stress field and can be reasonably considered constant at a

Mailing address: Dr. Antonio Emolo, Dipartimento di Scienze Fisiche, Università «Federico II», Complesso Universitario Monte S. Angelo, Via Cinthia, 80126 Napoli, Italy; e-mail: antonio.emolo@na.infn.it

large time scale. This idea is supported by several paleoseismic studies of active faults in different tectonic environments (*e.g.*, Pantosti and Valensise, 1990; Pantosti *et al.*, 1993; Meghraoui *et al.*, 2000). However, numerical simulations of the fracture development suggest that the fracture process may not repeat the same style of nucleation, propagation and arrest in successive rupture events along a given fault (Rice, 1993; Nielsen *et al.*, 1995; Cochard and Madariaga, 1996; Nielsen *et al.*, 2000).

Several authors have proposed different methods for simulating the seismic radiation associated with the rupture process along extended faults (Beroza and Spudich, 1988; Gariel and Campillo, 1989; Fäh and Suhadolc, 1994; Cotton and Campillo, 1995). We applied the method proposed by Zollo *et al.* (1997) for evaluating the strong motion parameters. It is a hybrid stochastic-deterministic method based on the massive computation of synthetic seismograms produced by a large number of different rupture processes occurring on a given fault. Each rupture process is simulated by adopting a kinematic description of the source and applying the self-similar *k-square* model (Herrero and Bernard, 1994) to distribute the final slip on the fault. Assuming a uniform rupture velocity, each rupture history is built from a heterogeneous final slip distribution and a random rupture nucleation point on the fault. Considering that the source effects are dominant at near source distances, the variability of synthetic strong motion records should account for the *a priori* unknown rupture complexity. The range of expected variation of typical strong motion parameters (PGA, PGV and spectral ordinates) for a given fault (or fault system) can therefore be estimated. This method has been previously applied to retrieve the expected PGA produced by a hypothetical $M = 7$ earthquake occurring on the Ibleo-Maltese fault system in South-Eastern Sicily (Zollo *et al.*, 1999a). The accuracy of the method was tested by comparing the predictive estimates with the empirical PGA attenuation curves (Sabetta and Pugliese, 1987). In this paper, we compare the accelerometric data recorded during the main shocks of the 1997 Umbria-Marche (Central Italy) seismic sequence with the synthetic estimates to verify the predictive method. The two main seismic events that occurred on September 26, 1997 (00:33 GMT, $M_w = 5.7$ and 09:40 GMT, $M_w = 6.0$) were recorded at several three-components accelerometric stations in the near source range. Table I lists the PGA values for the receivers considered in this study.

2. Modeling the ground acceleration field

The high frequency seismic radiation is controlled by the complexity and heterogeneity of the rupture process on the fault (Heaton, 1990;

Table I. PGA values recorded during the main shocks of the Umbria-Marche seismic sequence.

Station	PGA (m/s^2) September 26, 1997 00:33 earthquake	PGA (m/s^2) September 26, 1997 09:40 earthquake
Assisi	1.5	1.8
Bevagna	–	0.8
Castelnuovo	1.0	1.6
Cerreto di Spoleto	1.9	1.1
Colfiorito	3.6	2.9
Matelica	–	1.1
Monte Fiegni	0.2	–
Nocera Umbra	5.0	5.5

Anderson, 1991) in the near source distance range. The complexity of the faulting process largely dominates the character of the signal, when the site effects can be considered weak or negligible. When the dominant wavelengths are shorter than the minimum source-to-receiver distance, it is possible to consider the asymptotic solution of the wave equation as a good approximation of the near source wave field (Bernard and Madariaga, 1984; Farra *et al.*, 1986). The ground acceleration at the Earth surface associated with the wave phase c radiated by an extended fault Σ is given by the representation integral (Aki and Richards, 1980)

$$\ddot{u}_c(r;t) = \tag{2.1}$$

$$= \frac{\partial^2}{\partial t^2} \iint_{\Sigma} G_c^{FF}(r, r_0; t, 0) * \Delta\dot{u}(r_0; t - T_c) d\Sigma$$

where r and r_0 are, respectively, the positions of the receiver and of the elementary fault of area $d\Sigma$, $\Delta\dot{u}$ is the slip velocity function, T_c is the travel time and G_c^{FF} is the asymptotic Green's function. Following the approach of Farra *et al.* (1986), the Green's function for a direct body wave in a 1D elastic medium can be expressed as

$$G_c^{FF} = \frac{\mu_0}{4\pi\rho_0 c_0^3} \Re e\left[\sqrt{\frac{\rho_0 c_0}{\rho c J}} F_c \Pi\right] \delta(t - T_c) \tag{2.2}$$

where μ, ρ and c are, respectively, the shear modulus, the density and the wave velocity (the suffix 0 means evaluated at the source), J represents the geometrical spreading factor, F_c is the double-couple radiation pattern coefficient and Π contains the product of all the complex wave transmission coefficients at the different interfaces of the layered medium. In order to take into account of the anelasticity of the Earth, each Green's function is convolved with Azimi's attenuation function (Aki and Richards, 1980) parametrized by a constant quality factor Q_c.

The slip velocity function in eq. (2.1) is approximated by a box-car function

$$\Delta\dot{u}(r_0; t) = \tag{2.3}$$

$$= \begin{cases} \dfrac{D(r_0)}{\tau(r_0)} & \text{for } T_R(r_0) < t < T_R(r_0) + \tau(r_0) \\ 0 & \text{elsewhere} \end{cases}$$

where $T_R(r_0)$, $\tau(r_0)$ and $D(r_0)$ are, respectively, the rupture time, the rise time and the final slip associated with the fault element whose position is r_0. The representation integral is evaluated numerically by discretizing the fault Σ in subfaults and summing up the subfaults contribution.

Under a constant rupture velocity hypothesis, the *ω-square* behavior of the acceleration spectrum (Aki, 1967) can be related to self-similar slip and stress-drop distributions over the fault which follow a negative power-law of radial wave number k (Andrews, 1981; Frankel, 1991; Herrero and Bernard, 1994). We adopted the *k-square* model (Herrero and Bernard, 1994) for computing the final slip distribution on the fault plane. This distribution is obtained by the 2D inverse Fourier transform of the complex function

$$\Delta\tilde{u}(k_x, k_y) = C \frac{1}{1 + \left(\dfrac{k}{k_c}\right)^2} e^{i\Phi(k_x, k_y)} \tag{2.4}$$

where k is the radial wave number. The cut-off wave number k_c corresponds to the minimum fault dimension (Herrero and Bernard, 1994) and represents the characteristic dimension of the fault. The dislocation with wave number $k > k_c$ is supposed incoherent on the fault plane and the phase Φ is chosen randomly when $k > k_c$. The slip distribution is then tapered by using a two-dimensional cosine-taper filter in order to avoid unrealistic sharp slip transition at the fault edges. Finally, the constant C in the eq. (2.4) is evaluated by normalizing the slip distribution to obtain an *a priori* value of seismic moment.

In our simulation method we assume a constant rupture velocity. This means that the far-field radiation is dominated by the slip heterogeneities instead of the irregularities in the rupture front velocity. Our approximation may not be valid for highly discontinuous fracture phenomena but is reasonable when the rupture velocity varies smoothly on the fault.

The chosen rise time value is the cut-off frequency of the low-pass filter applied to the synthetic seismograms. Thus the onset of the slip appears as instantaneous at the passage of the rupture front. If the finite rise time τ was apparent, it would introduce a low-pass filtering effect on synthetics. Moreover, the choice of a negligible value of τ maximizes the expected amplitude of ground motion in the far-field approximation.

In order to avoid numerical effects due to the fault discretization (*e.g.*, spatial aliasing), a fine fault gridding is needed to simulate synthetics at frequencies up to 20 Hz. Zollo *et al.* (1997) suggest characteristic subfault dimensions of 20-30 m.

3. Source parameters for the September 26, 1997 Umbria-Marche main shocks

On September 26, 1997 Umbria-Marche region (Central Italy) was struck by two moderate size earthquakes (at 00:33 GMT, M_w = 5.7 and at 09:40 GMT, M_w = 6.0) which caused a few causalities and large building damages. The two main shocks were followed by an intense post-seismic activity that lasted several months and was characterized by hundreds of aftershocks, some of them with magnitudes in the range 4.5-5.4. This seismic sequence filled a gap in the area (Amato *et al.*, 1998). The focal mechanism for the two main shocks, evaluated by Ekström *et al.* (1998) applying the CMT technique on the long period data, are predominantly normal and the fault planes appear to be oriented in the typical NW-SE Apenninic direction.

Zollo *et al.* (1999b) and Capuano *et al.* (2000) used the strong motion data recorded at two near source stations (Assisi and Cerreto di Spoleto, fig. 1) in order to retrieve the source parameters for the two main shocks of the seismic sequence. The acceleration records were integrated and band-pass filtered in the 1-5 Hz frequency range. A first estimate of the apparent source duration at the Assisi station was obtained by applying the Empirical Green Function technique (Harztell, 1978). This was possible because the station Assisi recorded a small size foreshock (September 3, 1997, M_w = 4.5) located very close to the main shocks and characterized by a similar focal mechanism. The apparent source duration at the station Cerreto di Spoleto was roughly estimated on velocity records by measuring the time window containing the large amplitude *S*-wave motion. The *S*-wave polarization directions and the apparent source durations were then used to constrain fault geometry and mechanism for the two seismic events by comparing the observed and synthetic *S*-vector directions using a trial-and-error search technique. An estimate of the fault dimensions was inferred by plotting the *S*-wave isochrones on the fault plane (Zollo and Bernard, 1991). The isochrone is defined as

$$t^i = T^i_{0S} + \Delta t^i \qquad (3.1)$$

where T^i_{0S} and Δt^i are, respectively, the first *S* arrival time and the apparent source duration at the station *i*. The isochrone delimits the faulting area as seen from the station for a given rupture velocity (see fig. 3 in Zollo *et al.*, 1999b). The best estimate of the rupture area is determined by the intersection on the fault plane of all the isochrones (3.1) computed for all the available stations. The source parameters inferred by Zollo *et al.* (1999b) and Capuano *et al.* (2000) are reported in table II. The last step of the analysis consists in the waveform modeling. A trial-and error waveform modeling was applied to 1-5 Hz band pass filtered velocity records. The final slip distributions and the comparison between observed and synthetic velocity records are shown in fig. 1. The source parameters inferred by Zollo *et al.* (1999b) and Capuano *et al.* (2000) are well consistent with equivalent models obtained by modeling from SAR interferometry and GPS data (Stramondo *et al.*, 1999).

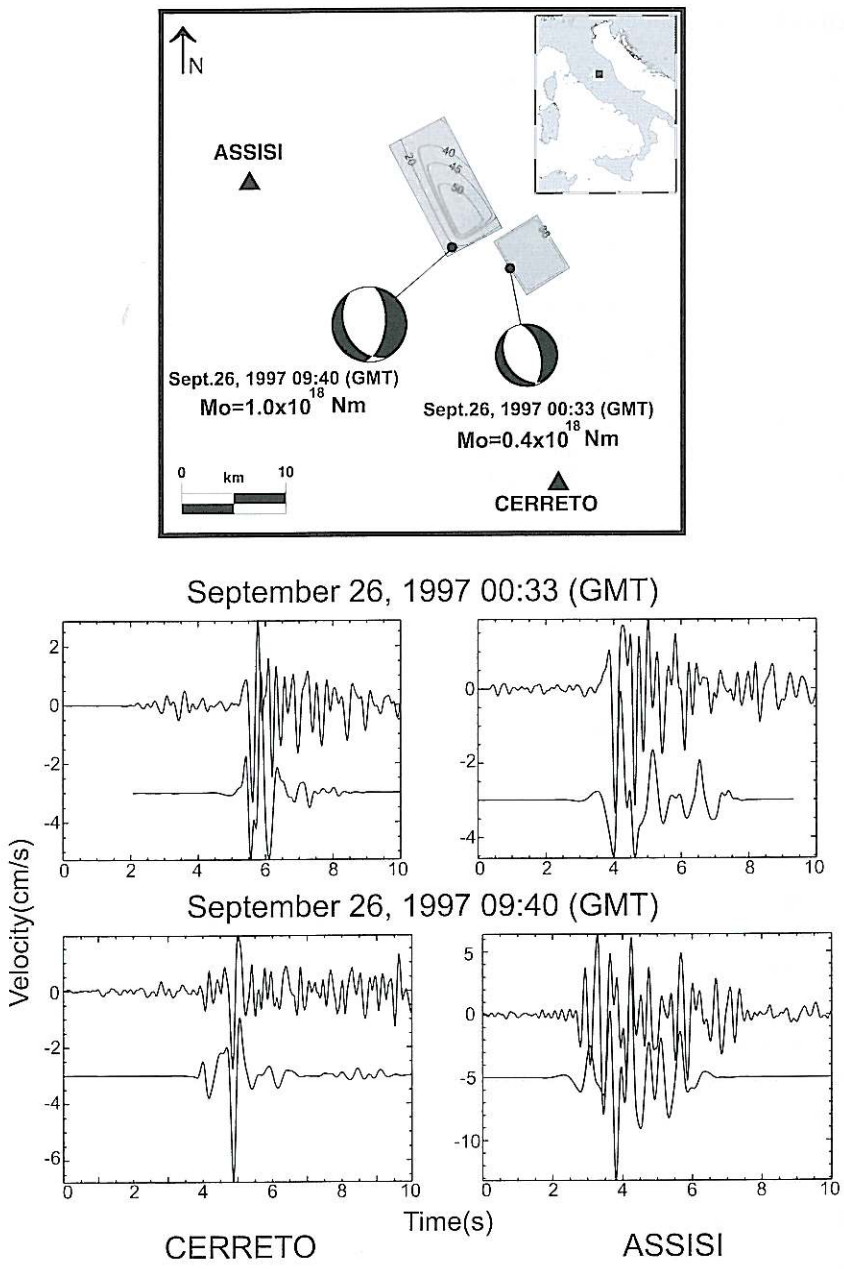

Fig. 1. *Top*: sketch of rupture model for the September 26, 1997, 00:33 GMT and 09:40 GMT events. The black dots indicate the position of the rupture nucleation point on the fault plane. Both rupture processes have been modeled using a constant rupture velocity. The heterogeneous final slip distribution for the 09:40 GMT event is shown on the fault plane. The fault parameters are given in table II. *Bottom*: comparison between observed and synthetic velocity records at Assisi and Cerreto di Spoleto for the September 26, 1997, 00:33 GMT and 09:40 GMT events. The traces are filtered in the 1-5 Hz frequency band. (Modified from Zollo *et al.*, 1999b).

4. Parameters for the simulation study

A grid of 121 receivers covering an area of 60 km^2 around the faults was used in our simulation study. The spacing between adjacent stations is 5 km (fig. 2).

One hundred different rupture processes were numerically reproduced for each analyzed event. The fault geometries, mechanisms and average slip were chosen according to the estimate of Zollo *et al.* (1999b). Each rupture process was characterized by a different final slip distribution (following the *k-square* model distribution in spectral domain) and by a rupture nucleation point randomly located on the fault plane. The fault planes were discretized by square subfaults with dimension 25×25 m^2. The rupture time of each subfault was computed assuming a constant rupture propagation velocity as reported in table II. The slip rise time was also assumed to be at a constant of 0.05 s for the two simulated events. This value corresponds to the short period limit chosen in our study because

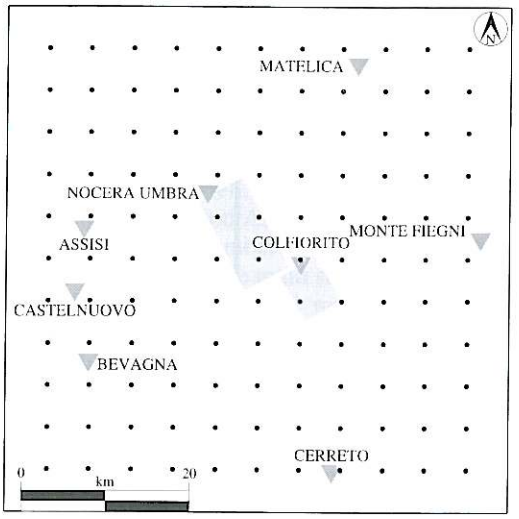

Fig. 2. Receiver configuration adopted in this simulation study (black circles). The gray rectangles represent the surface projection of the faults while the inverted triangles represent the real station locations with respect to the earthquakes sources.

Table II. Fault parameters used in this simulation study (after Capuano *et al.*, 2000).

Fault parameter	September 26, 1997 00:33 earthquake	September 26, 1997 09:40 earthquake
Strike	148°	152°
Dip	36°	38°
Rake	– 106°	– 118°
Length	6×10^3 m	12×10^3 m
Width	6×10^3 m	7.5×10^3 m
Bottom depth	7×10^3 m	8×10^3 m
Seismic moment	4×10^{19} N · m	9×10^{19} N · m
Average stress drop	1.9 MPa	1.5 MPa
Average final slip	0.38 m	0.37 m
Rupture velocity	3×10^3 m/s	2.6×10^3 m/s

Table III. Velocity model used in this simulation study (after Ponziani, 1994).

Depth (m)	v_p (m/s)	v_s (m/s)	ρ (kg/m^3)
0 – 200	2×10^3	1.1×10^3	2×10^3
200 – 1.8×10^3	4.4×10^3	2.4×10^3	2.4×10^3
1.8×10^3 – 8×10^3	5.9×10^3	3.2×10^3	2.4×10^3
8×10^3 – 15×10^3	6.25×10^3	3.5×10^3	2.5×10^3

we low-pass filtered our synthetics at 20 Hz. The synthetic accelerograms were then computed at the 121 stations for each simulated rupture process.

We only computed the acceleration field associated with the direct *S*-wave motion, assuming that it largely dominates in amplitude with respect to direct *P*-waves and converted/reflected waves in the near source distance range. The Green's functions for the direct *S* wave are computed by asymptotic ray approximation in the flat-layered velocity model proposed by Ponziani (1994) for the investigated area and reported in table III. A homogeneous Q_S value of 80 was used to compute the attenuation filter.

5. Estimate of strong motion parameters and comparison with the data

The mean value of PGA and the associated standard deviation of 100 simulations were computed at each receiver. Figures 3 and 5 show the maps of the mean values and the statistical coefficients of variation CoV ($\mathrm{CoV} = 100 \cdot \frac{\sigma_{<\mathrm{PGA}>}}{<\mathrm{PGA}>}$, where $<\mathrm{PGA}>$ represents the mean PGA value and $\sigma_{<\mathrm{PGA}>}$ the associated standard deviation) respectively, for the 00:33 GMT and for the 09:40 GMT earthquakes. The maps of mean values show radiation lobes due to the focal mechanisms. However, the map for the 00:33 GMT event shows dominant accelerations in the south-eastern sector while the map for the 09:40 GMT event shows dominant accelerations in the north-western sector. These trends are similar to those observed on the macroseismic fields for the two earthquakes (Tosi *et al.*, 1999) and are mainly related to a combined effect of source radiation pattern and geometry. In other words, there are some regions which could be struck more than others independently of the faulting process.

The interpretation of average PGA maps must be done considering the CoV maps. In fact, the maps of CoV express the normalized range of PGA variation due to the heterogeneity of the rupture process. Regions where CoV is higher suggest that PGA values can vary strongly depending on how the fracture nucle-

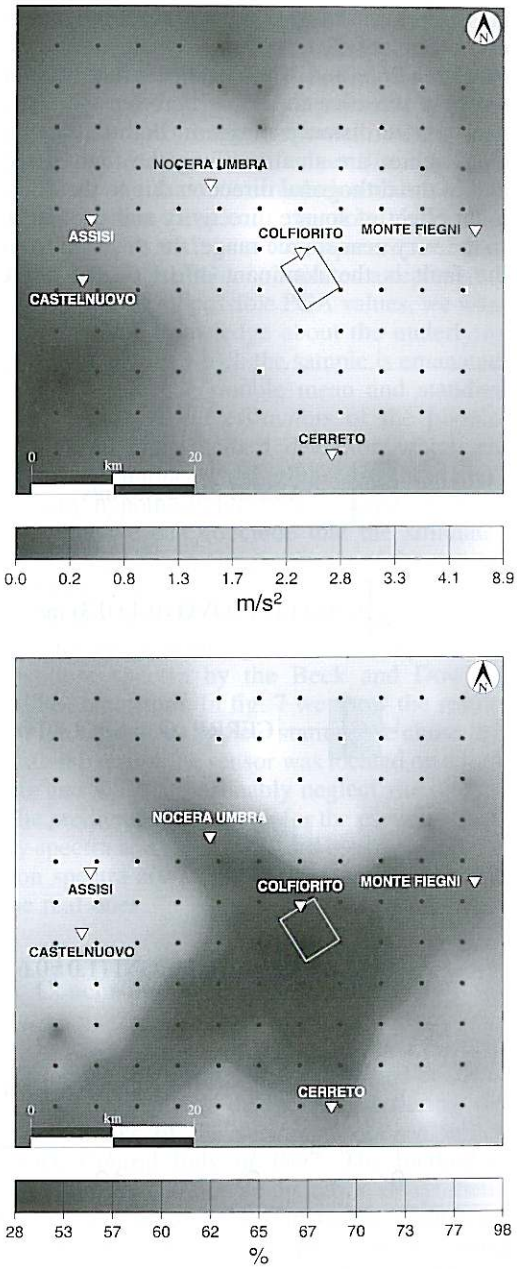

Fig. 3. *Top*: map of simulated peak ground acceleration (mean values from 100 simulations) for the September 26, 1997, 00:33 GMT event. *Bottom*: map of coefficient of variation CoV (see the text for its definition). The rectangle in the figures represent the surface projection of the fault.

ates, develops and stops during the faulting process. The relatively large values obtained for CoV (between 26% and 100%) indicate that PGA is strongly sensitive to source complexity in the near source distance range. In both cases, the CoV values are smaller along the fault strike and in the orthogonal direction due to the dominant effect of source directivity and geometry. In the very near source range, the distance from the fault is the dominant effect on the PGA values with respect to the heterogeneity of the source processes and this explain because in these regions we find smaller values for the CoV coefficient.

We compared the predicted PGA values with the data recorded at several accelerometric sites during the earthquakes. Figure 4 (for the 00:33 GMT event) and 6 (for the 09:40 GMT event) show the comparison between the predicted $[PGA_{min}, PGA_{MAX}]$ ranges with the observed PGA

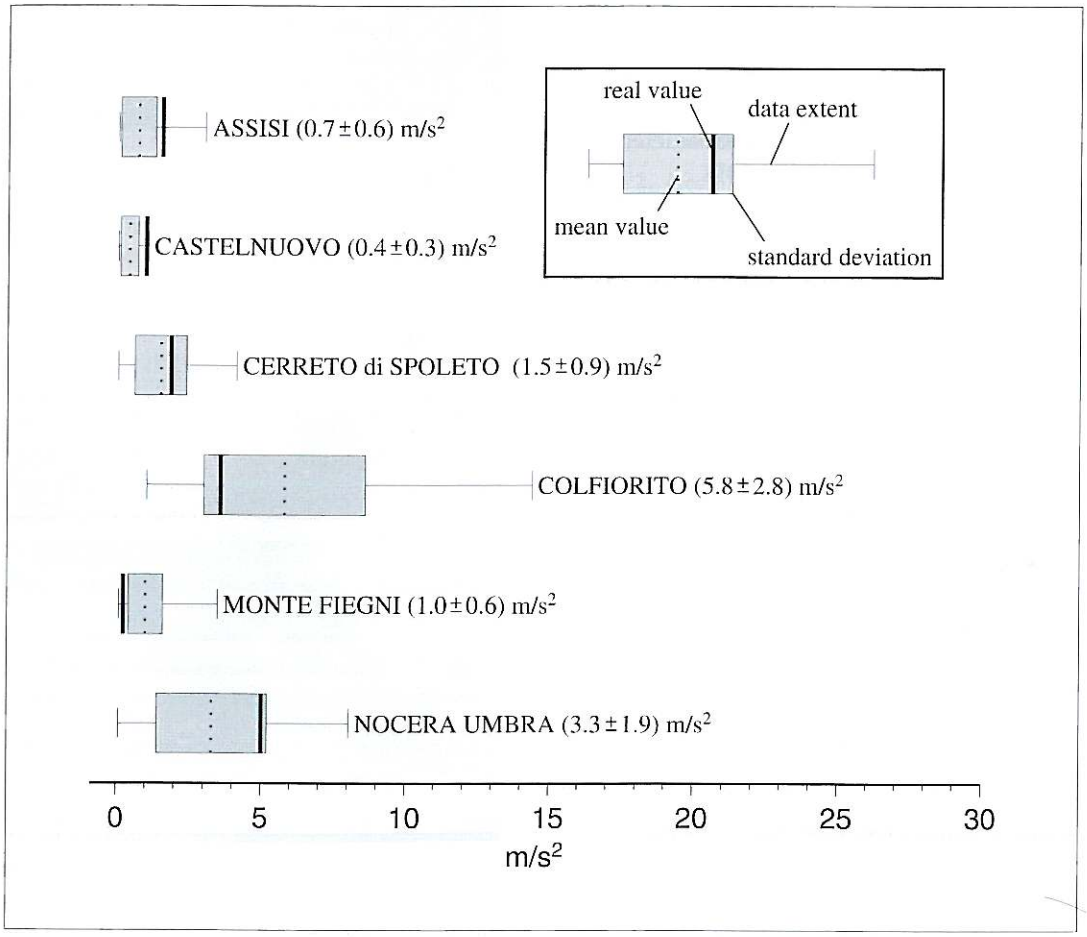

Fig. 4. Comparison between observed and simulated PGA valued for the September 26, 1997, 00:33 GMT event. The simulated mean value ± standard deviation computed from 100 simulations is also shown for each station. In the box in the upper right of the figures «data extent» corresponds to the range between the minimum simulated PGA and the maximum simulated PGA.

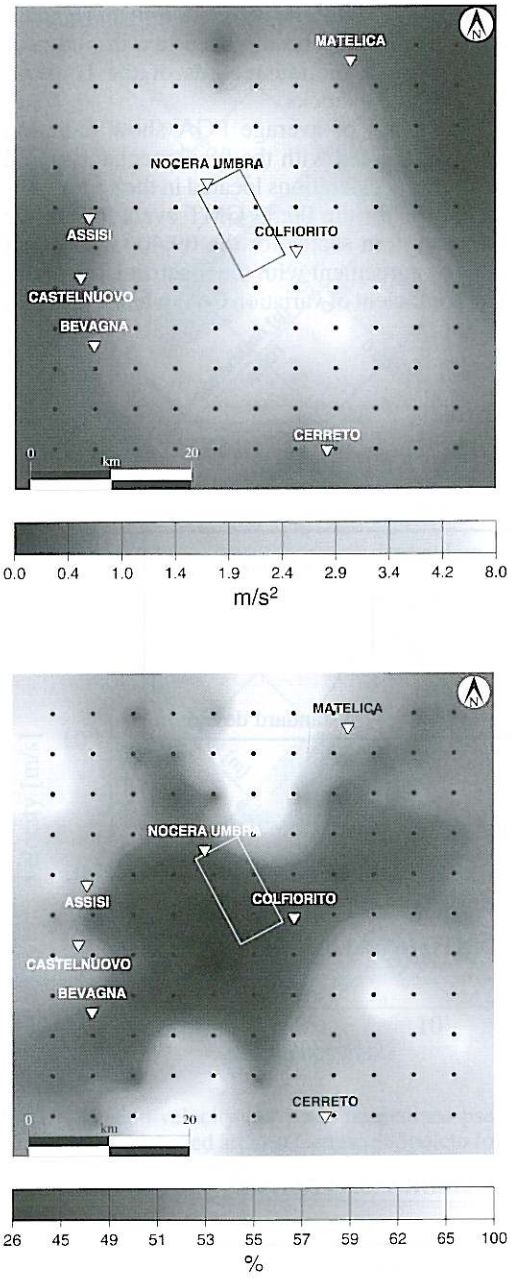

Fig. 5. Same as fig. 3 but for the September 26, 1997, 09:40 GMT event.

values. Again, the large range of the theoretical intervals shown in the figures is due to the variability of the simulated rupture processes. However, we find a satisfactory agreement between the predicted 1σ ranges (reported in figs. 4 and 6) and the measured PGA values (listed in table I). Assuming that our simulation data set is a representative sample of the possible rupture time histories and, as a consequence, our data set of simulated PGA constitutes a representative sample of all possible PGA values, we want to gain some knowledge about the underlying population from which the sample is emanated. In this sense, the sample mean and standard deviation represent estimators of the population mean and standard deviation which are consistent, unbiased and efficient, without making any hypothesis on the population distribution. So, we can conclude that the simulated 1σ intervals give a good estimate of the expected PGA ranges.

Finally, in order to test the spectral characteristics of the seismograms, we computed the response spectra by the Beck and Dowling (1988) algorithm. In fig. 7 we show the results for the Cerreto di Spoleto station. We chose this station because the sensor was located on a rock site and we can reasonably neglect site effects. The predicted ranges both for the pseudo-velocity spectra and the normalized pseudo-acceleration spectra are in satisfactory agreement with the real ones.

6. Conclusions

In this paper we applied the method for simulating the acceleration field proposed by Zollo *et al.* (1997) using data recorded during the main shocks of the seismic sequence which struck Central Italy in 1997. The method is based on the massive computation of synthetic records produced by a statistically significant number of possible rupture processes occurring on the same fault. The general idea underlying this approach is that, although the dynamic characteristics of the rupture process can change from a seismic event to another, the geometry, the mechanism and the average final slip on a given fault can be considered constant as they

are likely controlled by large scale tectonic stress. For each simulation, the rupture nucleation point was randomly variable on the entire fault and the final slip distribution on the fault was computed applying the *k-square* model (Herrero and Bernard, 1994). One hundred simulations were performed for each of the two largest seismic events and the associated synthetic accelerograms were computed at a network of 121 receivers covering an area of 60 km^2 around the faults. The source parameters used in this work were inferred by Zollo *et al.* (1999b) and Capuano *et al.* (2000) who modeled two digital near source strong motion records of the Umbria-Marche main shocks.

The maps of average PGA show radiation lobes associated with the focal mechanism and dominant accelerations located in the south-eastern sector for the 00:33 GMT event and in the north-western sector for the 09:40 GMT event in good agreement with the macroseismic field. The coefficient of variation CoV, which expresses

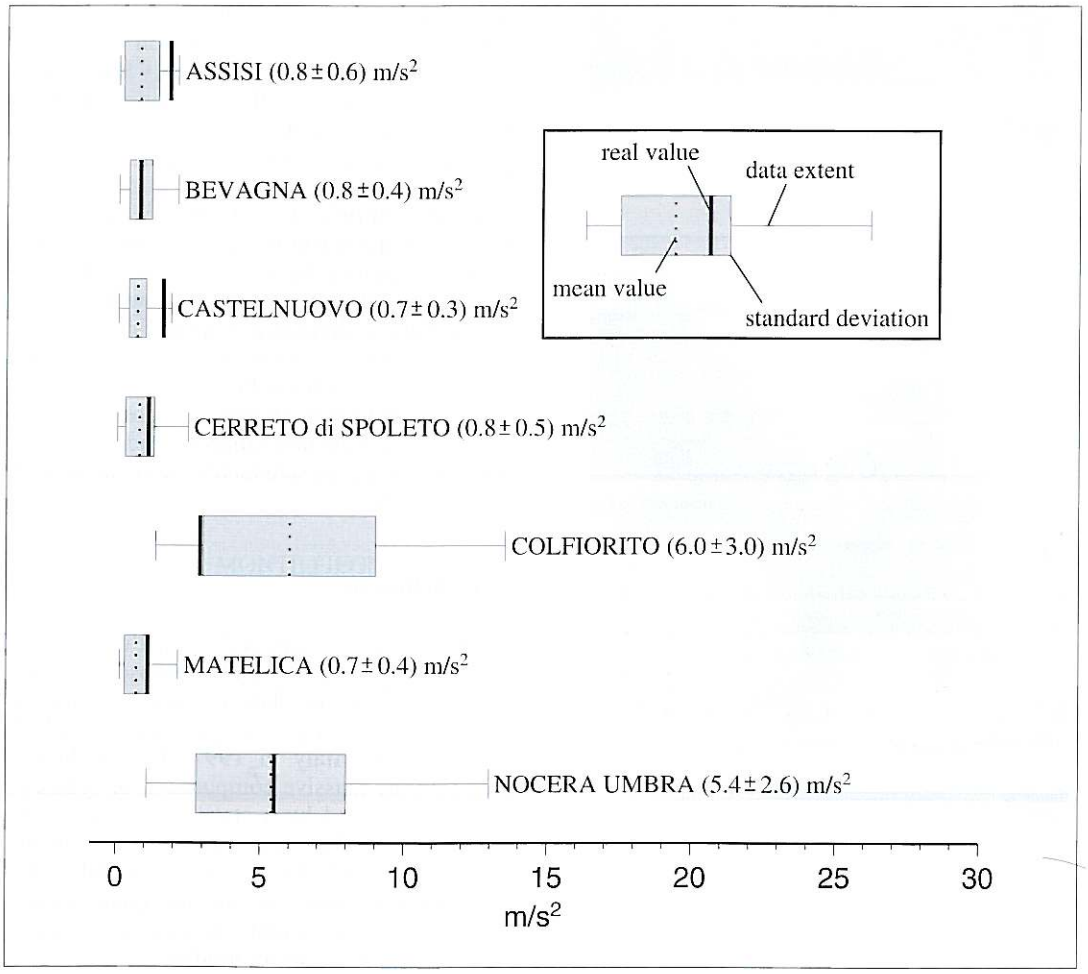

Fig. 6. Same as fig. 4 but for the September 26, 1997, 09:40 GMT event.

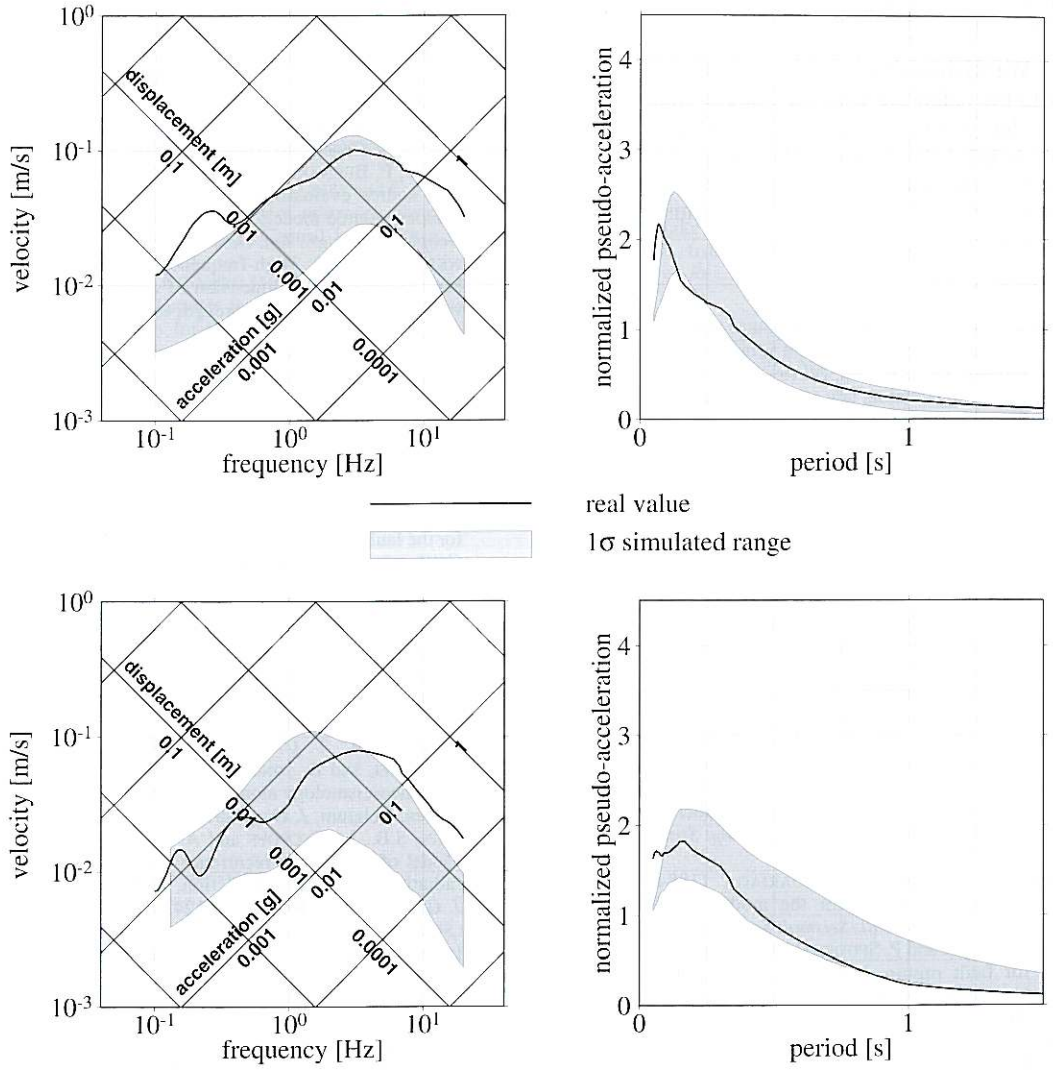

Fig. 7. Pseudo-velocity (*left*) and normalized pseudo-acceleration (*right*) spectra recorded (continuous line) and simulated (shaded area) at Cerreto di Spoleto for the September 26, 1997, 00:33 GMT event (*top*) and for the 09:40 GMT event (*bottom*).

the variability of estimated peak acceleration caused by the source complexity, is smaller along the approximate directions NW-SE and NE-SW due to the dominant effect of source directivity and geometry. The comparison of observed and synthetic data, both in time and in frequency domains, shows that the predictive method provides a satisfactory estimate of the acceleration field due to the two earthquakes in the near source range where the complexity of the rupture process strongly influences the seismic radiation.

Acknowledgements

We wish to thank S. Marcucci and G. Milana who provided the Umbria-Marche main shocks accelerograms data set, A. Herrero and S. Nielsen for helpful discussions. We are grateful to M. Cocco and an anonymous reviewer for their constructive comments on the manuscript.

REFERENCES

ABRAHAMSON, N.A. and K.M. SHEDLOCK (1997): Some comparisons between recent ground-motion relations. *Seismol. Res. Lett.*, **68**, 24-40.

AKI, K. (1967): Scaling law of seismic spectra. *J. Geophys. Res.*, **72**, 1217-1231.

AKI, K. and P.G. RICHARDS (1980): *Quantitative Seismology, Theory and Methods* (W.H. Freeman and Co., San Francisco, U.S.A.), vols. 1 and 2, pp. 932.

AMATO, A., R. AZZARA, C. CHIARABBA, G.B. CIMINI, M. COCCO, M. DI BONA, L. MARGHERITI, S. MAZZA, F. MELE, G. SELVAGGI, A. BASILI, E. BOSCHI, F. COURBOULEX, A. DESCHAMPS, S. GAFFET, G. BITTARELLI, L. CHIARALUCE, D. PICCININI, and M. RIPEPE (1998): The 1997 Umbria-Marche, Italy, earthquake sequence: a first look at the main shocks and aftershocks. *Geophys. Res. Lett.*, **25**, 2861-2864.

ANDERSON, J.G. (1991): Strong motion seismology. *Rev. Geophys., Supplement*, 700-720.

ANDREWS, D.J. (1981): A stochastic fault model, 2. Time-independent case. *J. Geophys. Res.*, **86**, 10821-10834.

BECK, J.L. and M.J. DOWLING (1988): Quick algorithms for computing either displacement, velocity or acceleration of an oscillator, *Earthquake Eng. Struct. Dyn.*, **16**, 245-253.

BERNARD, P. and R. MADARIAGA (1984): A new asymptotic method for the modeling of near-field accelerograms, *Bull. Seismol. Soc. Am.*, **74**, 539-555.

BEROZA, G.C. and P. SPUDICH (1988): Linearized inversion for fault rupture behavior: application to the 1984 Morgan Hill, California, earthquake, *J. Geophys. Res.*, **93**, 6275-6296.

BOORE, D.M., W.B. JOYNER and T.E. FUMAL (1997): Empirical near-source attenuation relationships for horizontal and vertical components of peak ground acceleration, peak ground velocity and pseudo-absolute acceleration response spectra, *Seismol. Res. Lett.*, **68**, 154-179.

CAPUANO, P., A. ZOLLO, A. EMOLO, S. MARCUCCI and G. MILANA (2000): Rupture mechanism and source parameter of Umbria-Marche main shocks from strong motion data, *J. Seismol.*, **4**, 463-478.

COCHARD, A. and R. MADARIAGA (1996): Complexity of seismicity due to highly rate-dependent friction, *J. Geophys. Res.*, **101**, 25321-25336.

COTTON, F. and M. CAMPILLO (1995): Frequency domain inversion of strong ground motions: applications to the 1992 Landers, California earthquake, *J. Geophys. Res.*, **100**, 3961-3965.

EKSTRÖM, G., A. MORELLI, E. BOSCHI and A.M. DZIEWONSKI (1998): Moment tensor analysis of the Central Italy earthquake sequence of September-October 1997, *Geophys. Res. Lett.*, **25**, 1971-1974.

FÄH, D. and P. SUHADOLC (1994): Application of numerical wave propagation techniques to study local soil effects: the case of Benevento (Italy), *Pageoph*, **143**, 513-536.

FARRA, V., P. BERNARD and R. MADARIAGA (1986): Fast near source evaluation of strong ground motion for complex source models, in *Earthquake Source Mech., Geophys. Monogr., Am. Geophys. Un.*, **37**, 121-130.

FRANKEL, A. (1991): High-frequency spectral falloff of earthquakes, fractal dimension of complex rupture, *b* value, and the scaling of strength on fault, *J. Geophys. Res.*, **96**, 6291-6302.

GARIEL, J.C. and M. CAMPILLO (1989): The influence of the source on the high-frequency behavior of the near-field acceleration spectra: a numerical study, *Geophys. Res. Lett.*, **16**, 279-282.

HARTZELL, S. (1978): Earthquake aftershock as Green's functions, *Geophys. Res. Lett.*, **5**, 1-4.

HARTZELL, S. and T.H. HEATON (1983): Inversion of strong-ground motion and teleseismic waveforms data for the fault rupture history of the 1979 Imperial Valley, California earthquake, *Bull. Seismol. Soc. Am.*, **73**, 1553-1583.

HEATON, T.H. (1990): Evidence for and implications of self-healing pulses of slip in earthquake rupture, *Phys. Earth Planet. Inter.*, **64**, 1-20.

HERRERO, A. and P. BERNARD (1994): A kinematic self-similar rupture process for earthquakes. *Bull. Seismol. Soc. Am.*, **84**, 1216-1229.

MEGHRAOUI, M., T. CAMELBEECK, K. VANNESTE, M. BRONDEEL and D. JONGMANS (2000): Active faulting and paleoseismology along the Bree fault, lower Rhine graben, Belgium, *J. Geophys. Res.*, **105**, 13809-13841.

NIELSEN, S.B., L. KNOPOFF and A. TARANTOLA (1995): Model of earthquake recurrence: role of elastic wave radiation, relaxation of friction, and inhomogeneity, *J. Geophys. Res.*, **100**, 12423-12430.

NIELSEN, S.B., J.M. CARLSON and K.B. OLSEN (2000): Influence of friction and fault geometry on earthquake rupture, *J. Geophys. Res.*, **105**, 6069-6088.

PANTOSTI, D. and G. VALENSISE (1990): Faulting mechanism and complexity of the November 23, 1980, Campania-Lucania earthquake, inferred from surface observations, *J. Geophys. Res.*, **95**, 15319-15341.

PANTOSTI, D., D. SCHWARTZ and G. VALENSISE (1993): Paleoseismicity along the 1980 surface rupture of the Irpinia fault: implications for earthquake recurrence in the Southern Apennines, Italy, *J. Geophys. Res.*, **98**, 6561-6577.

PONZIANI, F. (1994): Digitalizzazione e reinterpretazione di dati di sismica crostale: ipotesi su un modello geodinamico per l'Italia Centrale - Tirreno Settentrionale, *Ph.D. Thesis*, University of Perugia, Italy.

RICE, J.R. (1993): Spatio-temporal complexity of slip on fault, *J. Geophys. Res.*, **98**, 9885-9907.

SABETTA, F. and A. PUGLIESE (1987): Attenuation of peak horizontal acceleration and velocity from Italian strong-motion records, *Bull. Seismol. Soc. Am.*, **77**, 1491-1513.

STRAMONDO, S., M. TESAURO, P. BRIOLE, E. SANSOSTI, S. SALVI, R. LANARI, M. ANZIDEI, D. BALDI, G. FORNARO, A. AVALLONE, M.F. BUONGIORNO, G. FRANCESCHETTI and E. BOSCHI (1999): The September 26, 1997, Colfiorito, Italy, earthquakes: modeled coseismic surface displacement from SAR interferometry and GPS, *Geophys. Res. Lett.*, **26**, 883-887.

TOSI, P., A. TERTULLIANI, V. DE RUBEIS and C. GASPARINI (1999): Preliminary results of macroseismic survey of the Colfiorito sequence (Central Italy), *Phys. Chem. Earth*, **24**, 477-481.

ZOLLO, A. and P. BERNARD (1991): How does an asperity break? New elements from the waveform inversion of accelerograms for the 2319 UT, October 15, 1979, Imperial Valley aftershocks, *J. Geophys. Res.*, **96**, 21549-21573.

ZOLLO, A., A. BOBBIO, A. EMOLO, A. HERRERO and G. DE NATALE (1997): Modeling of ground acceleration in the near source range: the case of 1976, Friuli earthquake (M = 6.5), Northern Italy, *J. Seismol.*, **1**, 305-319.

ZOLLO, A., A. EMOLO, A. HERRERO and L. IMPROTA (1999a): High frequency strong ground motion modeling in the Catania area associated with the Ibleo-Maltese fault system, *J. Seismol.*, **3**, 279-288.

ZOLLO, A., S. MARCUCCI, G. MILANA and P. CAPUANO (1999b): The 1997 Umbria-Marche (Central Italy) earthquake sequence: insights on the main shock ruptures from near source strong motion records, *Geophys. Res. Lett.*, **26**, 3165-3168.

(received January 15, 2001;
accepted May 29, 2001)